Experimental Neurology 312 (2019) 1–9

Contents lists available at ScienceDirect

Experimental Neurology

journal homepage: www.elsevier.com/locate/yexnr

Research Paper

Denervated mouse dentate granule cells adjust their excitatory but not inhibitory synapses following *in vitro* entorhinal cortex lesion

Maximilian Lenz[a,b,1], Christos Galanis[a,1], Dimitrios Kleidonas[a], Meike Fellenz[b], Thomas Deller[b], Andreas Vlachos[a,*]

[a] Department of Neuroanatomy, Institute of Anatomy and Cell Biology, Faculty of Medicine, University of Freiburg, Freiburg 79104, Germany
[b] Institute of Clinical Neuroanatomy, Neuroscience Center, Goethe-University Frankfurt, Frankfurt 60590, Germany

ARTICLE INFO

Keywords:
Homeostatic synaptic plasticity
Synaptic scaling
Inhibition
GABA
Gephyrin
Organotypic slice cultures

SUMMARY

Neurons adjust their synaptic strength in a homeostatic manner following changes in network activity and connectivity. While this form of plasticity has been studied in detail for excitatory synapses, homeostatic plasticity of inhibitory synapses remains not well-understood. In the present study, we employed entorhinal cortex lesion (ECL) of organotypic entorhino-hippocampal tissue cultures to test for homeostatic changes in GABAergic neurotransmission onto partially denervated dentate granule cells. Using single and paired whole-cell patch-clamp recordings, as well as immunostainings for synaptic markers, we find that excitatory synaptic strength is robustly increased 3 days post lesion (dpl), whereas GABAergic neurotransmission is not changed after denervation. Even under conditions of pharmacological inhibition of glutamatergic neurotransmission, which prevents neurons to compensate for the loss of input *via* excitatory synaptic scaling, down-scaling of GABAergic synapses does not emerge 3 days after denervation. We conclude that granule cells maintain structural and functional properties of GABAergic synapses even in the face of substantial changes in network connectivity. Hence, alterations in inhibitory neurotransmission, as seen in pathological brain states, may not simply reflect a homeostatic response to disconnection.

1. Introduction

Neurons adjust their structural and functional properties in response to perturbations in network activity (*e.g.*, Luscher and Malenka, 2012; Bliss and Collingridge, 2013; Granger and Nicoll, 2014). In recent years, several mechanisms have been identified that aim at maintaining neurons in a stable state (Davis, 2006; Marder and Goaillard, 2006; Turrigiano, 2011, 2017). One of the best studied mechanisms is homeostatic synaptic plasticity, which adjusts synaptic strength in a compensatory manner (Turrigiano, 2008). While pharmacologic and genetic approaches have been employed to perturb network activity in order to study the cellular and molecular mechanisms of homeostatic synaptic plasticity, its significance under pathological conditions is still debated (Small, 2008; Hulme et al., 2013; Maggio and Vlachos, 2014).

It is well accepted that neurons respond to denervation with structural and functional changes that partially compensate for the denervation effects (Steward, 1994). In earlier work we were able to demonstrate that neurons which lose part of their input after traumatic injury, *i.e.*, following *in vitro* entorhinal cortex lesion, increase their excitatory synaptic strength in a homeostatic manner (*e.g.*, Vlachos et al., 2012a). Interestingly, these changes occur predominantly in the denervated zone, *i.e.*, on distal dendritic segments which lose most of their excitatory input and remodel their dendritic spines (Vlachos et al., 2012b). Consistent with this observation, recent *in vivo* findings confirm the existence of local homeostatic excitatory synaptic plasticity, which accompanies lesion-induced spine remodeling (Barnes et al., 2017). Although changes of GABAergic synapses have been reported in the context of denervation [*e.g.* (Simbürger et al., 2000, 2001; Maffei et al., 2006; van Versendaal et al., 2012; Kinuchi et al., 2018)], it remains unclear whether homeostatic changes in GABAergic neurotransmission, as described for TTX-treated dissociated neuron preparations (Turrigiano, 2011), accompany denervation-induced local excitatory synaptic strengthening.

Considering the relevance of inhibition under physiological and pathological conditions (Letzkus et al., 2015; Tremblay et al., 2016; Tatti et al., 2017), we here employed *in vitro* entorhinal cortex lesion to test for homeostatic scaling of GABAergic neurotransmission onto denervated dentate granule cells. In this model the entorhino-

* Corresponding author.
E-mail address: andreas.vlachos@anat.uni-freiburg.de (A. Vlachos).
[1] ML and CG contributed equally to this work.

https://doi.org/10.1016/j.expneurol.2018.10.013
Received 23 July 2018; Received in revised form 16 October 2018; Accepted 23 October 2018
Available online 25 October 2018
0014-4886/

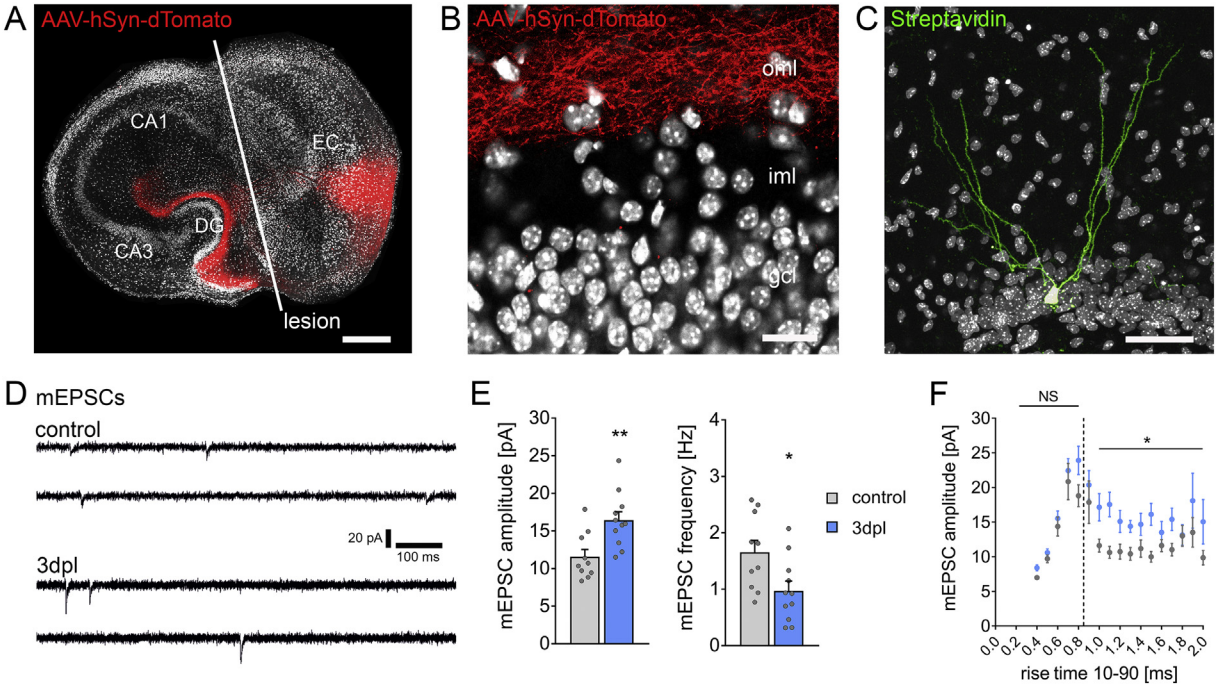

Fig. 1. *In vitro* denervation induces an increase in excitatory synaptic strength.
(A) Overview of a mouse organotypic entorhino-hippocampal slice culture stained with nuclear stain (white) to visualize cytoarchitecture. The entorhino-hippocampal projection is visualized by AAV-hSyn-dTomato expression in the entorhinal cortex (EC). At 18–21 days *in vitro* the entorhino-hippocampal projection is dissected without directly damaging the target neurons in the dentate gyrus (DG). Scale bar = 300 µm. (B) The dentate gyrus at higher magnification. Note dTomato-stained fibers in the outer molecular layer (oml). Scale bar = 20 µm. gcl: granule cell layer; iml: inner molecular layer. (C) Example of a recorded, biocytin-filled and post-hoc stained dentate granule cell (Streptavidin; green). Scale bar = 50 µm. (D) Sample traces of AMPA receptor-mediated miniature excitatory postsynaptic currents (mEPSCs) recorded from dentate granule cells in non-denervated controls and age- and time-matched denervated tissue cultures 3 days post lesion (dpl). (E) A significant increase in mean mEPSC amplitude and a reduction in mean mEPSC frequency are observed (control, $n = 10$ cells; denervated, $n = 11$ cells; Mann-Whitney test, U-values ≤ 21). (F) Sorting of mEPSC events by rise time reveals a significant difference in amplitudes between control and denervated dentate granule cells for events with a rise time ≥ 0.85 ms. Shorter rise times do not show significant differences between the groups (statistical comparisons made between mean values of events < 0.85 and ≥ 0.85 per cell; Mann-Whitney test, U-value = 19). Individual data points are indicated by gray dots. Values represent mean ± s.e.m. (** $P < .01$; * $P < .05$; NS, non-significant differences).

hippocampal projection can be dissected without directly damaging the target neurons (Fig. 1A-C). This leads to the partial denervation of dentate granule cells in the outer molecular layer (Fig. 1B, C). Using this *in vitro* model, we addressed the hypothesis that (1) partially denervated neurons respond with a homeostatic decrease in inhibitory synaptic strength, which accompanies the compensatory increase in excitatory neurotransmission, and that (2) inhibitory neurotransmission changes predominantly on denervated dendrites.

2. Materials and methods

2.1. Ethics statement

Mice were maintained in a 12 h light/dark cycle with food and water available *ad libitum*. Every effort was made to minimize distress and pain of animals. All experimental procedures were performed according to the German animal welfare legislation and approved by the appropriate animal welfare committee and/or the animal welfare officer at Goethe-University Frankfurt, Faculty of Medicine, and Albert-Ludwigs-University Freiburg, Faculty of Medicine.

2.2. Preparation of slice cultures

Entorhino-hippocampal tissue cultures were prepared at postnatal day 4–5 from *C57BL/6 J* and *GAD65-GFP* (heterozygous for GFP; Lopez-Bendito et al., 2004) mice of either sex. Cultivation medium contained 50% (*v*/v) MEM, 25% (v/v) basal medium eagle, 25% (v/v) heat-inactivated normal horse serum, 25 mM HEPES buffer solution, 0.15% (*w/v*) bicarbonate, 0.65% (w/v) glucose, 0.1 mg ml^{-1} streptomycin, 100 U ml^{-1} penicillin, and 2 mM glutamax. The pH was adjusted to 7.3, and the medium was replaced three times per week. All slice cultures were allowed to mature for at least 18 days in humidified atmosphere with 5% CO_2 at 35 °C. Complete transection of the perforant path (Fig. 1A) was ensured by removing the entorhinal cortex. All experiments were performed at 3 days post lesion (dpl) and/or corresponding age- and time-matched 4-week-old non-denervated control cultures.

2.3. Pharmacology

In some experiments slice cultures were treated with CNQX (50 µM) and APV (50 µM) for 3 days to block α-amino-3-hydroxy-5-methyl-4-isoxazolepropionic acid (AMPAR) and N-Methyl-D-aspartate (NMDAR) receptors, respectively. Treatment started immediately after the lesion. Age- and time-matched non-denervated control cultures were treated in the same way, except for entorhinal cortex lesion.

2.4. Perforant path tracing

Adeno-associated viruses (AAV) obtained from SignaGen Laboratories, Maryland (AAV2-Synapsin-tdTOMATO, catalog #SL100896) were injected into the entorhinal cortex at 3–5 days *in vitro* at a Zeiss Axioscope 2 equipped with a 4× objective (air, NA 0.1) using borosilicate glass pipettes. Cultures were returned to the incubator immediately after injection and allowed to mature for at least 18 days in humidified atmosphere with 5% CO_2 at 35 °C.

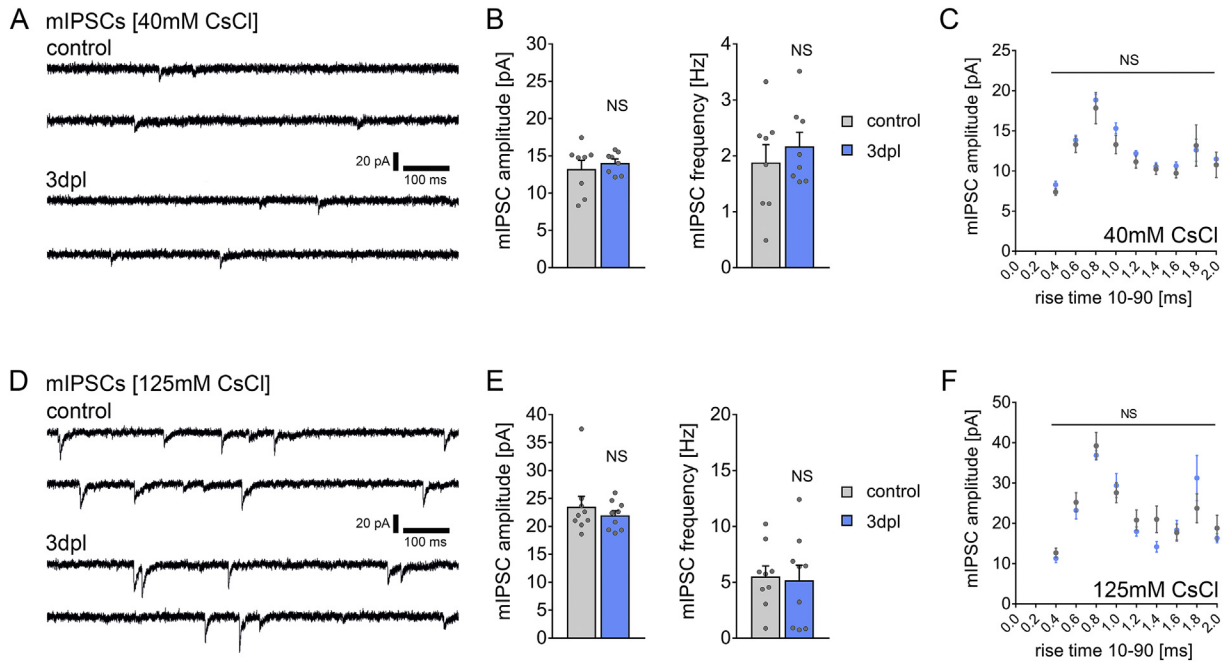

Fig. 2. Homeostatic down-scaling of GABAergic synapses does not occur during denervation-induced excitatory synaptic strengthening.
(A) Sample traces of $GABA_A$ receptor-mediated miniature inhibitory postsynaptic currents (mIPSCs) recorded from dentate granule cells in non-denervated controls and age- and time-matched denervated tissue cultures 3 days post lesion (dpl) using 40 mM CsCl-containing internal solution. (B) Mean mIPSC amplitude and frequency are not significantly different between the two groups (control, $n = 8$ cells; denervated, n = 8 cells; Mann-Whitney test). (C) Sorting mIPSC events by rise time does not reveal any significant differences between the groups (Two-Way-ANOVA with Bonferroni post-hoc correction for multiple testing). (D-F) In an independent set of non-denervated and denervated tissue cultures, mIPSC recordings were carried out using 125 mM CsCl-containing internal solution. No significant differences between the two groups were observed in these experiments (control, $n = 9$ cells; denervated, n = 9 cells). Individual data points are indicated by gray dots. Values represent mean ± s.e.m. (NS, non-significant differences).

2.5. Post-hoc staining

Cultures were fixed in a solution of 4% (*w/v*) paraformaldehyde (PFA) in phosphate-buffered saline (PBS, 0.1 M, pH 7.4) and 4% (w/v) sucrose for 1 h. Fixed cultures were incubated for 1 h with 10% (*v*/v) normal goat serum (NGS) in 0.5% (v/v) Triton X-100-containing PBS. Biocytin filled cells were counterstained with Alexa488-conjugated Streptavidin (Invitrogen; 1:1000; in PBS with 10% NGS, 0.1% Triton X-100) for 4 h and DAPI staining was used to visualize cytoarchitecture (1:5000; in PBS for 10 min). Slices were washed, transferred and mounted onto glass slides for visualization. Streptavidin stained granule cells were visualized with a Leica TCS SP8 laser scanning confocal microscope equipped with a 40× oil immersion objective lens (NA 1.3).

2.6. Immunostaining and imaging

Slice cultures were fixed in a solution of 4% (w/v) PFA in PBS (0.1 M, pH 7.4) and 4% (w/v) sucrose for 1 h, followed by 2% (w/v) PFA and 30% (w/v) sucrose in PBS overnight. Cryostat sections (30 µm) of fixed slice cultures were prepared, and stained with antibodies against $GABA_A$R-α2 (Santa Cruz Biotech., sc-7350; 1:500), gephyrin (Synaptic Systems, clone mAb7a; 1:500), and parvalbumin (Swant, PV-28; 1:200) following a modified protocol previously described (Lenz et al., 2016). Briefly, sections were incubated for 1 h with 10% (*v*/v) normal goat serum (NGS) or normal horse serum (NHS) in 0.5% (v/v) Triton X-100-containing PBS to reduce unspecific staining and subsequently incubated for 48 h at 4 °C with the respective primary antibodies (in PBS with 10% NGS or NHS and 0.1% Triton X-100). Sections were washed and incubated for 3 h with appropriate Alexa488- or 568-labeled secondary antibodies (Invitrogen; 1:1000, in PBS with 10% NGS or NHS, 0.1% Triton X-100). TO-PRO® (Invitrogen) or DAPI nuclear stain was used to visualize cytoarchitecture (1:5000; in PBS for 10 min). Sections were washed, transferred onto glass slides and mounted for visualization with anti-fading mounting medium.

Confocal images were acquired using a Nikon Eclipse C1si laser-scanning microscope with a 4× objective lens (NA 0.2, Nikon), a 20× objective lens (NA 0.9, Nikon), and a 60× oil-immersion objective lens (NA 1.4, Nikon). Three visual fields per region of interest were imaged in each culture at high magnification. Detector gain and amplifier were initially set to obtain pixel intensities within a linear range.

2.7. Whole-cell patch-clamp recordings

Whole-cell voltage-clamp recordings from dentate granule cells of slice cultures were carried out at 35 °C (2–5 neurons per culture). The bath solution contained 126 mM NaCl, 2.5 mM KCl, 26 mM $NaHCO_3$, 1.25 mM NaH_2PO_4, 2 mM $CaCl_2$, 2 mM $MgCl_2$, and 10 mM glucose. For mEPSC recordings patch pipettes contained 126 mM K-gluconate, 4 mM KCl, 4 mM Mg-ATP, 0.3 mM Na_2-GTP, 10 mM PO-creatine, 10 mM HEPES, and 0.1% biocytin (pH = 7.25 with KOH, 290 mOsm with sucrose). For mIPSC recordings patch pipettes contained 40 mM CsCl, 90 mM K-gluconate, 1.8 mM NaCl, 1.7 mM $MgCl_2$, 3.5 mM KCl, 0.05 mM EGTA, 2 mM Mg-ATP, 0.4 mM Na_2-GTP, 10 mM PO-Creatine, 10 mM HEPES (pH = 7.25 with KOH, 290 mOsm with sucrose) or 125 mM CsCl, 5 mM NaCl, 2 mM $MgCl_2$, 2 mM Mg-ATP, 0.5 mM Na_2-GTP, 0.1 mM EGTA, and 10 mM HEPES (pH = 7.33 with CsOH; 274 mOsm with sucrose) having a tip resistance of 4–6 MΩ. Spontaneous IPSCs (sIPSCs) were recorded with 125 mM CsCl containing internal solution. Alexa488 or Alexa568 (both 10 µM) was added to the internal solution in some experiments to visualize neuronal morphology prior to recordings. For mIPSC and mEPSC recordings neurons were recorded at a holding potential of −70 mV in the presence of 0.5 µM TTX and 10 µM APV. For mIPSC recordings 10 µM CNQX was added to the bath solution as well. sIPSC recordings were performed in the presence of APV and CNQX (both 10 µM), but without adding TTX to the bath solution. Series resistance was monitored in

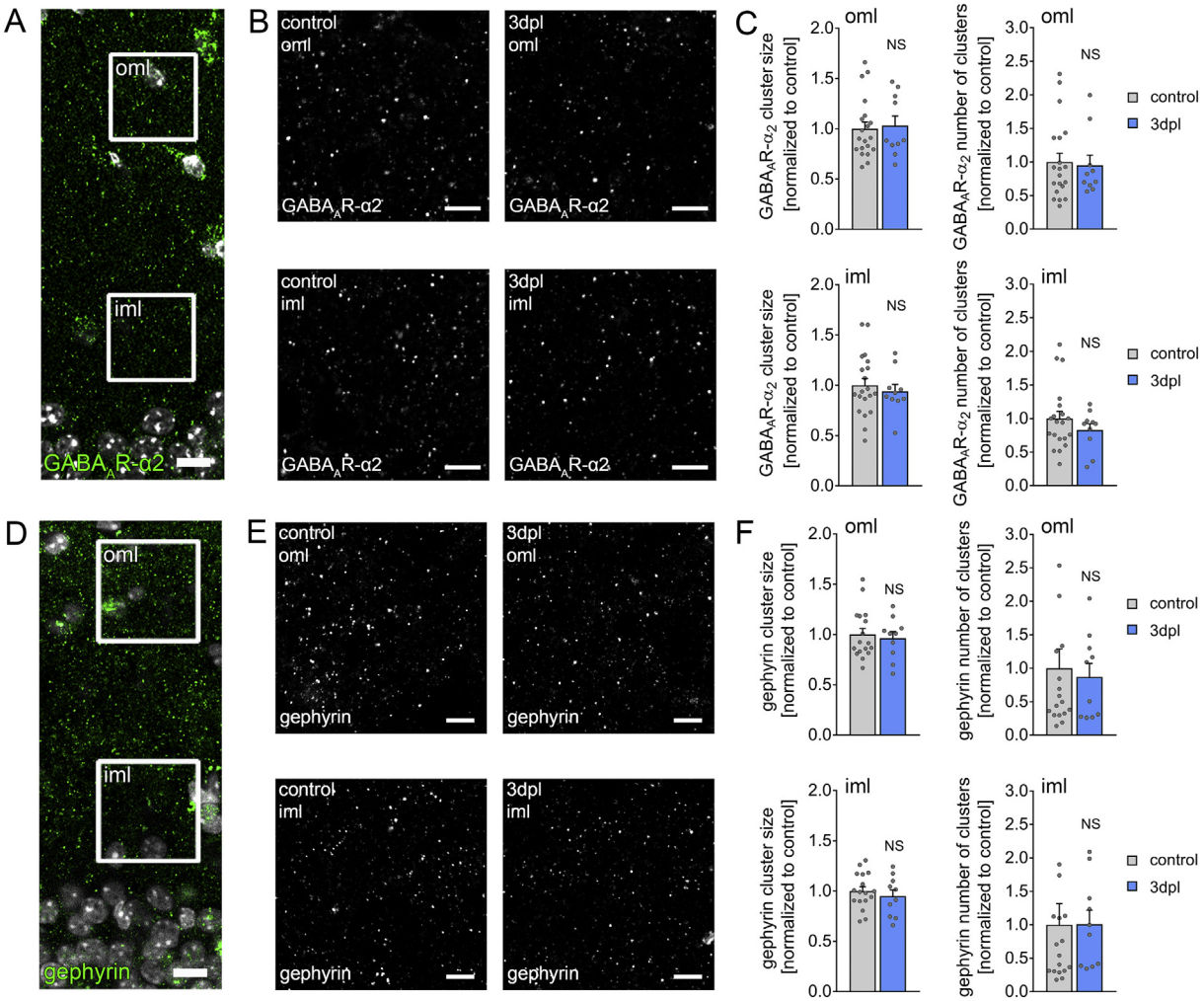

Fig. 3. No changes in $GABA_A$ receptor (subunit α2) and gephyrin clusters 3 days after *in vitro* denervation.
(A-C) Slice cultures stained for $GABA_A$ receptors (subunit α2; green). Cluster sizes and numbers assessed in the outer (oml) and inner molecular layer (iml) of the dentate gyrus. Three visual fields were imaged at higher magnification per region of interest and slice culture. No significant differences in $GABA_A$R-α2 cluster sizes and numbers were observed between non-denervated controls and age- and time-matched denervated tissue cultures at 3 days post lesion (control, $n = 20$ cultures; denervated, n = 10 cultures; Mann-Whitney test). White, TO-PRO nuclear stain. Scale bars = 10 µm (A) and 4 µm (B). (D-F) A different set of cultures was stained for the postsynaptic scaffolding protein gephyrin (green). Cluster sizes and numbers assessed as described above. No significant differences between the two groups were detected in these experiments (control, $n = 17$ cultures; denervated, n = 10 cultures; Mann-Whitney-test; one value outside the axis limits in the control group for number of clusters in OML and in IML). Scale bars = 10 µm (D) and 4 µm (E). Individual data points are indicated by gray dots. Values represent mean ± s.e.m. (NS, non-significant differences).

2 min intervals, and recordings were discarded, if leak current or series resistance changed significantly and/or reached ≥ 30 MΩ.

2.8. Paired recordings

Simultaneous whole-cell patch-clamp recordings of neurons were carried out as described previously (Lenz et al., 2016). Slice cultures prepared from *GAD65-GFP* mice were used to readily identify interneurons projecting their axons onto dendrites of dentate granule cells, respectively. Internal solution for presynaptic recordings of GFP-expressing interneurons contained 126 mM K-gluconate, 4 mM KCl, 4 mM Mg-ATP, 0.3 mM Na_2-GTP, 10 mM PO-creatine, 10 mM HEPES, and 0.1% biocytin (pH = 7.25 with KOH, 290 mOsm with sucrose). Postsynaptic dentate granule cells were recorded with an internal solution containing 125 mM CsCl, 5 mM NaCl, 2 mM $MgCl_2$, 2 mM Mg-ATP, 0.5 mM Na_2-GTP, 0.1 mM EGTA, and 10 mM HEPES (pH = 7.33 with CsOH; 274 mOsm with sucrose) at a holding potential of −70 mV. Action potentials were generated by 3 ms square current pulses (1 nA) elicited at 0.2 Hz (up to 50 pulses), while recording inhibitory postsynaptic currents from dentate granule cells (recordings performed in the presence of APV and CNQX, both 10 µM. For short-term plasticity, 5 action potentials were applied at 20 Hz (inter-sweep-interval: 5 s; 30 repetitions).

2.9. Quantification and statistics

Analysis was performed by investigators blind to experimental conditions. Electrophysiological data were analyzed using pClamp 10.6 (Axon Instruments) and MiniAnalysis (Synaptosoft) software. 150–350 mIPSC/sIPSC or mEPSC events were analyzed per recorded neuron. Rise time analysis was performed using rise 10–90 [ms] of single mEPSC or mIPSC/sIPSC events. Mean amplitude [pA] per rise time was calculated by matching amplitude and rise 10–90 with a rise time bin of 0.1 or 0.2, respectively.

Paired recordings were manually assessed using pClamp 10.6 (Axon Instruments). Network connectivity was estimated by calculating the ratio between connected pairs and the total number of probed pairs. The percentage of action potentials not successfully evoking

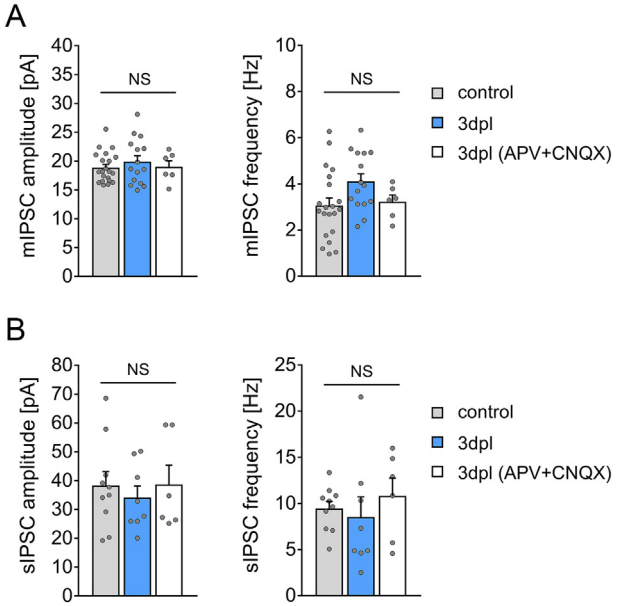

Fig. 4. *In vitro* denervation does not affect GABAergic neurotransmission in presence of glutamate receptor blockers.
(A, B) AMPA receptors and NMDA receptors were pharmacologically blocked with CNQX (50 μM) and APV (50 μM), respectively. No significant differences in miniature and spontaneous inhibitory postsynaptic currents (A, mIPSC; B, sIPSC) were detected in these experiments. APV- + CNQX-treated non-denervated controls and age- and time-matched untreated controls were pooled, since no significant differences were detected between the groups (mIPSCs: control, $n = 21$ cells; denervated, $n = 15$ cells; denervated (APV + CNQX), $n = 6$ cells. sIPSCs: control, n = 10 cells; denervated, n = 8 cells; denervated (APV + CNQX), n = 6 cells. Kruskal-Wallis test followed by Dunn's post-hoc correction). Individual data points are indicated by gray dots. Values represent mean ± s.e.m. (NS, non-significant differences).

Table 1
Pharmacological inhibition of AMPA receptors with CNQX (50 μM) and NMDA receptors with APV (50 μM) does not alter $GABA_AR$-α2 and gephyrin cluster sizes in the inner molecular layer (iml) and outer molecular layer (oml) 3 days post lesion (dpl). $n = 5$ cultures in each group, Mann-Whitney-test. Values represent mean ± s.e.m., normalized to non-denervated control cultures.

Cluster size	control		3 dpl (APV + CNQX)	
	iml	oml	iml	oml
$GABA_AR$-α2	1.0 ± 0.09	1.0 ± 0.04	0.84 ± 0.07	0.98 ± 0.12
Gephyrin	1.0 ± 0.15	1.0 ± 0.06	1.13 ± 0.11	1.09 ± 0.07

postsynaptic current responses was determined (synaptic failure rate), as well as the mean amplitude of all successfully evoked postsynaptic responses. Amplitudes of postsynaptic responses were normalized to the first pulse in averaged traces of short-term plasticity recordings. Sizes and numbers of immunolabeled $GABA_AR$-α2 and gephyrin clusters were assessed using the Image-J software package (available from http://rsb.info.nih.gov/ij) as previously described (Vlachos et al., 2013b). Data were analyzed using GraphPad Prism 7 (GraphPad software, USA). Mann-Whitney test (to compare two groups) or the Kruskal-Wallis test followed by Dunn's post-hoc test (for multiple comparisons) were used. For evaluation of mIPSC rise time analysis, two-way-ANOVA following Bonferroni's post-hoc correction was performed. *P*-values of $< .05$ were considered a significant difference. All values represent mean ± standard error of the mean. In the figures * denotes $P < .05$ and ** $P < .01$; non-significant differences are indicated with 'NS'. Single data points are indicated by gray dots. U-values provided for significant results in the figure captions.

2.10. Digital illustrations

Confocal image stacks were stored as TIF files. Figures were prepared using Photoshop graphics software (Adobe, San Jose, CA, USA). Image brightness and contrast were adjusted.

3. Results

3.1. Entorhinal cortex lesion in vitro induces a compensatory increase in excitatory synaptic strength

Individual dentate granule cells were patched, and AMPAR-mediated miniature excitatory postsynaptic currents (mEPSCs) were recorded from denervated and age- and time-matched non-denervated controls (at 3 dpl; Fig. 1). A significant increase in mean mEPSC amplitude and a reduction in mEPSC frequency were observed in the denervated group (Fig. 1D, E). This result is in line with our earlier findings on a denervation-induced compensatory increase in excitatory synaptic strength, which accompanies the reduction in spine synapse numbers following *in vitro* entorhinal cortex lesion (*e.g.*, Vlachos et al., 2013a).

In order to test whether all excitatory synapses of a denervated neuron respond equally, we sorted mEPSC events by rise time, as the rise time of mEPSCs can be used to determine the distance of synapses from the soma of patched neurons (*e.g.*, Soltesz et al., 1995; Wierenga and Wadman, 1999; Letzkus et al., 2006; Sjostrom and Hausser, 2006; Williams and Mitchell, 2008; Peng et al., 2009; Lenz et al., 2015). In our previous work we used computational modeling and local electrical stimulation to confirm that mEPSC events with a rise time ≥ 0.85 ms originate from synapses on dendrites in the outer molecular layer, *i.e.*, the layer which is partially denervated (Vlachos et al., 2012a). Indeed, this analysis revealed that events with a rise time ≥ 0.85 ms show a significant difference in mEPSC amplitudes between lesioned and non-lesioned cultures, whereas events with a faster rise time derived from synapses close to the soma do not show significant differences (Fig. 1F). These findings confirm that *in vitro* entorhinal cortex lesion induces an increase in excitatory synaptic strength on distal granule cell dendrites.

3.2. Changes in GABAergic synaptic strength are not observed 3 days following in vitro entorhinal cortex lesion

In a different set of experiments, we tested for changes in GABAergic synaptic strength following *in vitro* entorhinal cortex lesion. Granule cells were patched, and $GABA_A$ receptor-mediated miniature inhibitory postsynaptic currents (mIPSCs) were recorded (Fig. 2). No significant differences in mean mIPSC amplitude and frequency were observed between the two groups at 3 dpl. To test for local adaptation in inhibition, which may have escaped the statistical assessment of mean values, rise time analysis of mIPSC events was performed. No significant differences between the groups were observed (Fig. 2A-C).

In an independent set of experiments, we used high-chloride internal solution to increase the sensitivity of our mIPSC recordings (Fig. 2D-F). Again, no significant differences in mIPSC amplitude and frequency were detected between the groups. We conclude that denervation-induced excitatory synaptic strengthening (c.f., Fig. 1) is not accompanied by major functional changes in GABAergic synaptic strength at 3 dpl.

3.3. $GABA_A$ receptor-α2 and gephyrin cluster properties are not changed in the denervated zone 3 days following in vitro entorhinal cortex lesion

Our previous work established a close interrelation between functional changes in GABAergic neurotransmission and $GABA_A$ receptor-α2 cluster properties in entorhino-hippocampal slice cultures (Lenz et al., 2016). Hence, to confirm and extend our mIPSC findings slice cultures were immunostained for $GABA_AR$-α2 subunits. As shown in

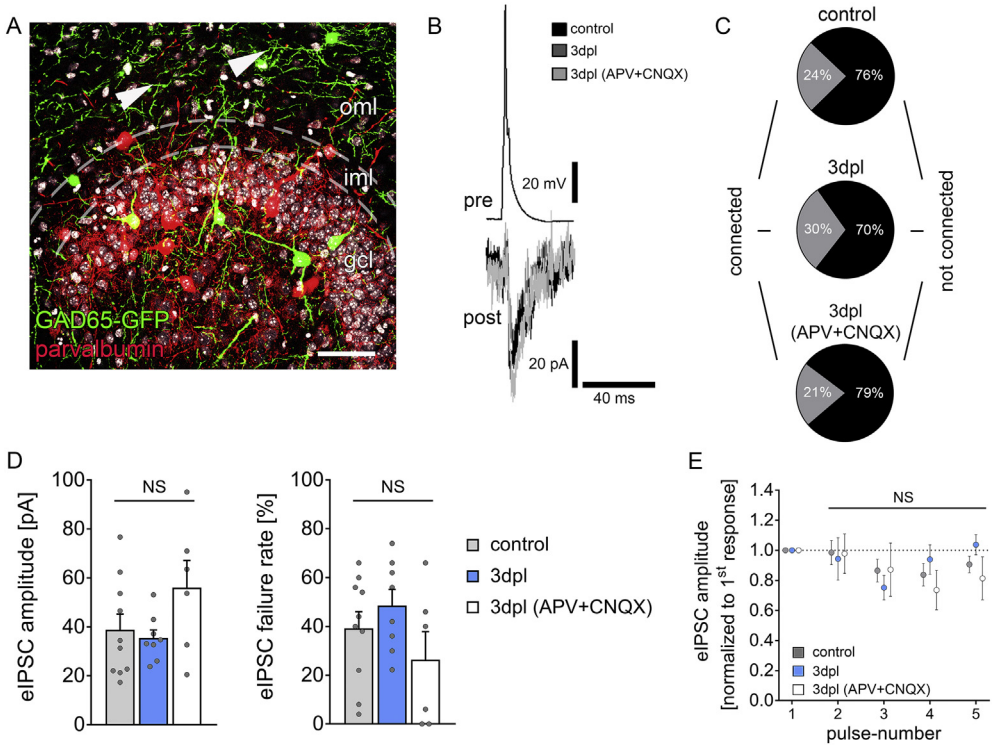

Fig. 5. No differences in GABAergic synaptic strength, efficacy and connectivity 3 days after *in vitro* denervation.
(A) A slice culture prepared from *GAD65-GFP* mice (green), stained for parvalbumin (red) is shown. GFP-expressing interneurons in the hilar region do not express parvalbumin and project mainly into the outer molecular layer (oml; arrowheads point to GFP-labeled axons) of the dentate gyrus. Note parvalbumin signal in the granule cell layer (gcl). White, TO-PRO nuclear stain. Scale bar = 100 µm. (B) Example of successfully evoked time-locked postsynaptic currents from dentate granule cells. Up to 50 action potentials were induced at 0.2 Hz in presynaptic GFP-expressing interneurons while recording from postsynaptic granule cells. (C-D) No changes in the probability to find connected pairs (C) and evoked IPSC (eIPSC) amplitude and failure rates are observed between the groups [control: 10 connected/41 probed pairs; denervated (3 dpl): 8 connected/27 probed pairs; denervated (3 dpl, APV + CNQX): 6 connected/28 probed pairs]. (E) Short-term plasticity was tested by inducing five action potentials at 20 Hz. The amplitude of each consecutive inhibitory postsynaptic current is normalized to the amplitude of the first response. No significant difference between non-denervated controls, age- and time-matched denervated tissue cultures, both untreated and pharmacologically treated (APV + CNQX, 50 µM each), was observed [control: 10 pairs; denervated (3 dpl): 8 pairs; denervated (3 dpl, APV + CNQX): 6 pairs; Kruskal-Wallis test, followed by Dunn's post-hoc correction]. Individual data points are indicated by gray dots. Values represent mean ± s.e.m. (NS, non-significant differences).

Fig. 3A-C, no significant differences in $GABA_AR$-α2 cluster properties were detected between the two groups at 3 dpl. Specifically, in the denervated outer molecular layer (oml) cluster sizes and numbers remained unchanged (Fig. 3C).

Similar results were obtained when cultures were stained for gephyrin (Vlachos et al., 2013c), which is the major postsynaptic scaffolding protein to which $GABA_A$ receptors anchor (Essrich et al., 1998, Feng et al., 1998; Kneussel et al., 1999; Fig. 3D-F). Together with our mIPSC recordings we conclude that no major functional or structural reorganization of GABAergic postsynapses occurs in dentate granule cells 3 days after *in vitro* entorhinal cortex lesion.

3.4. Pharmacological inhibition of glutamatergic synapses of denervated granule cells does not trigger changes in GABAergic neurotransmission

Based on the results obtained above, we speculated that the adjustment of excitatory synapses may suffice to compensate for the denervation-induced loss of input. Hence, changes in GABAergic neurotransmission may not be required to compensate for *in vitro* entorhinal cortex lesion. To address this issue, entorhinal cortex lesion and pharmacological inhibition of glutamatergic neurotransmission were combined to hinder denervated neurons from compensating *via* excitatory synaptic scaling. We speculated that under this experimental condition a compensatory reduction in GABAergic synaptic strength might emerge.

AMPARs and NMDARs were pharmacologically blocked with CNQX [50 µM] and APV [50 µM] immediately after denervation (for 3 days), and mIPSCs were recorded from dentate granule cells. Fig. 4 shows no significant changes in mIPSC properties in these experiments. Also, APV- + CNQX-treatment of non-denervated control cultures had no significant effect on mIPSC amplitudes and frequencies ($n_{untreated\ control}$ = 15 cells, $n_{control\ (APV+CNQX)}$ = 6 cells; mIPSC amplitude: untreated control, 18.5 ± 0.58 pA; control (APV + CNQX), 19.8 ± 1.4 pA; Mann-Whitney test, p = .42; mIPSC frequency: untreated control, 2.9 ± 0.4 Hz; control (APV + CNQX), 3.4 ± 0.5 Hz; Mann-Whitney test, p = .52). Similar results were obtained for $GABA_AR$-α2 and gephyrin immunostainings (Table 1). Hence, GABAergic synaptic strength is not adjusted in a homeostatic manner, even when the adjustment of excitatory neurotransmission at 3 dpl does not compensate for the denervation-induced loss of input.

3.5. Spontaneous GABAergic postsynaptic currents are not changed 3 days after denervation

We also recorded spontaneous IPSCs (sIPSCs) from denervated and non-denervated granule cells to test whether compensatory changes occur at the level of spontaneous network activity (Fig. 4B). No significant differences between the groups were observed at 3 dpl. Also, pharmacological inhibition of glutamatergic neurotransmission in denervated cultures did not alter mean sIPSC amplitude and frequency (Fig. 4B).

3.6. Paired recordings of dendritically projecting hilar inhibitory interneurons and dentate granule cells

Finally, paired whole-cell patch-clamp recordings of hilar interneurons and dentate granule cells were performed to probe inhibitory neurotransmission onto distal granule cell dendrites in the OML at the level of individual connected pairs of neurons. Hilar interneurons were readily identified by their GFP expression in slice cultures prepared from *GAD65-GFP* mice (Fig. 5A, B).

The results can be summarized as follows: (1) The probability to find connected pairs of neurons did not change 3 days after denervation (Fig. 5C), (2) no significant differences in evoked IPSC amplitudes were observed (Fig. 5D), (3) synaptic failure rates, *i.e.*, the number of action potentials not evoking IPSCs in connected pairs of neurons, were not

significantly different (Fig. 5D), and (4) short-term plasticity (5 pulses at 20 Hz) was not significantly different between the two groups (Fig. 5E). The data were also compared to a third group of denervated and APV- + CNQX-treated cultures, which were recorded in parallel: no significant changes in GABAergic neurotransmission were obtained in this group as well (c.f., Fig. 5B-E). All together, we are confident to conclude that unlike excitatory synaptic strength at 3 dpl, GABAergic synapses are not adjusted in a homeostatic manner in denervated cultured dentate granule cells.

4. Discussion

In this study, we tested whether homeostatic changes of GABAergic neurotransmission accompany denervation-induced excitatory synaptic plasticity. To this end, the well-established *in vitro* entorhinal cortex lesion model was employed. While the previously reported compensatory increase in excitatory synaptic strength was readily seen 3 days after denervation (c.f., Vlachos et al., 2012a), we were not able to detect corresponding changes, *i.e.*, down-scaling of GABAergic neurotransmission on partially denervated dentate granule cells; both at the functional and structural level. Also, pharmacological inhibition of glutamatergic neurotransmission had no major effect on GABAergic neurotransmission in non-denervated and denervated cultures. These results demonstrate that dentate granule cells maintain their *GABAergic synaptic set-point*, while adjusting excitatory synapses in response to major changes in network connectivity, *i.e.*, *in vitro* lesion-induced deafferentation.

Work from recent years has shed new light on the role of inhibitory neurotransmission in complex brain function (Griffen and Maffei, 2014; Caroni, 2015; Froemke, 2015; Letzkus et al., 2015; Tremblay et al., 2016). Studies employing optogenetic approaches demonstrate the relevance of local inhibitory networks in neural function and plasticity. It was shown, for example, that a transient reduction in local network inhibition mediates learning and memory (Letzkus et al., 2011; Pi et al., 2013; Wolff et al., 2014; Fu et al., 2015). These studies confirm and extend previous work demonstrating that decreased inhibition improves learning (Collinson et al., 2002; Botta et al., 2015), while increased GABAergic neurotransmission impairs learning and memory formation (Davis, 1979; Sanger and Joly, 1985; McNaughton and Morris, 1987; Brioni et al., 1989; Arolfo and Brioni, 1991; Harris and Westbrook, 1995). Consistent with these results, alterations in inhibitory neurotransmission have been linked to pathological brain states (Steinberg et al., 2015), such as schizophrenia (Yizhar et al., 2011; Rowland et al., 2013), autism spectrum disorders (Rubenstein and Merzenich, 2003; Rojas et al., 2014), panic disorders (Long et al., 2013) and epilepsy (Peng et al., 2013; Gu et al., 2017; Bui et al., 2018).

In earlier work changes in $GABA_AR$-α2 and gephyrin immunoreactivity were assessed following *in vivo* entorhinal denervation (Simbürger et al., 2000, 2001). These *in vivo* studies focused on the sprouting response occurring at later time points rather than on homeostatic changes occurring during the first days post lesion. Simbürger and colleagues demonstrated an increase of $GABA_AR$-α2 and gephyrin immunoreactivity after one week of denervation, most likely reflecting sprouting of GABAergic fibers (Deller et al., 1995) and reactive synaptogenesis onto denervated granule cells. A slight reduction in gephyrin immunoreactivity was reported 2 days after denervation (Simbürger et al., 2000), which the authors attributed to the loss of GABAergic entorhino-hippocampal projections (Germroth et al., 1989, 1991; see also Melzer et al., 2012). In line with our results, another study focusing on homeostatic plasticity of CA1 pyramidal neurons (Dinocourt et al., 2011) reported no changes in $GABA_AR$-α1, vGAT and GAD67 expression within 14 days after *in vivo* Schaffer collateral lesion (c.f., Simbürger et al., 2001). These studies corroborate our major conclusion that denervation does not trigger a homeostatic GABAergic down-scaling response. Hence, alterations in GABAergic neurotransmission - as seen under pathological *in vivo* conditions (Lewis, 2014; Radhu et al., 2015; Kiss et al., 2016) - may not simply reflect a homeostatic adjustment of inhibition in response to disconnection. Strikingly, GABAergic neurotransmission is kept constant also under conditions in which glutamatergic neurotransmission is pharmacologically blocked (both in non-denervated and denervated slice cultures). It is therefore conceivable that (1) mechanisms exist which maintain *GABAergic synaptic set-points* (by preventing their homeostatic adjustment), and/or (2) additional (pathological) stimuli are required for structural and functional homeostatic plasticity of GABAergic synapses to occur.

In our previous work we were able to show that homeostatic plasticity of inhibitory neurotransmission can be induced in entorhino-hippocampal slice cultures (Vlachos et al., 2013c). In the presence of the allosteric $GABA_A$ receptor agonist diazepam, a compensatory reduction in inhibitory neurotransmission was observed in CA1 pyramidal neurons of 4-week-old slice cultures (Vlachos et al., 2013c). Consistent with these functional changes, diazepam also caused a destabilization of gephyrin clusters. Interestingly, treatment with TTX had no apparent effects on gephyrin (Vlachos et al., 2013c), suggesting that changes in network activity *per se* are not sufficient to trigger compensatory changes of inhibition. Instead, changes in GABAergic neurotransmission (and/or signals affecting interneuron function) might be required. These findings strengthen the case for specific signals and molecular pathways regulating synaptic scaling of inhibition.

The pro-inflammatory cytokine tumor necrosis factor (TNF) mediates excitatory synaptic scaling (Stellwagen and Malenka, 2006; Steinmetz and Turrigiano, 2010) and down-regulates inhibitory neurotransmission (Pribiag and Stellwagen, 2014). Since TNF-signaling pathways have been linked to denervation-induced plasticity (Becker et al., 2013, 2015; Barnes et al., 2017), we expected a reduction in inhibitory neurotransmission in the denervated zone, which is characterized by increased TNF levels (Becker et al., 2013). Because we did not observe changes in inhibitory neurotransmission in the present study, it is unlikely that TNF coordinates homeostatic changes of excitatory and inhibitory neurotransmission in our experimental setting, *i.e.*, excitatory synaptic up-scaling and inhibitory synaptic down-scaling; at least not in granule cells 3 days after *in vitro* entorhinal cortex lesion.

Indeed, it has been recently shown that distinct mechanisms mediate homeostasis at excitatory and inhibitory synapses. For example, CaMKIV-/pCREB-mediated homeostatic mechanisms account for compensatory changes in excitatory synaptic strength (and intrinsic cellular properties), while changes in inhibitory neurotransmission do not depend on CaMKIV and pCREB (Joseph and Turrigiano, 2017). Likewise, Clptm1 affects $GABA_A$ receptors without changing AMPAR-mediated currents (Ge et al., 2018). While it remains to be shown whether (i) the recruitment of calcineurin-dependent phosphatases (Bannai et al., 2009; Lenz et al., 2016) and/or calcium-dependent serine proteases (Tyagarajan et al., 2013) is required for a down-regulation of GABAergic neurotransmission, and (ii) changes of GABAergic synapses may occur at later time points after denervation (c.f., Simbürger et al., 2000, 2001; Kinuchi et al., 2018), at this point we can state with confidence that *in vitro* entorhinal cortex lesion (and/or pharmacological inhibition of glutamatergic neurotransmission) is not sufficient to induce homeostatic synaptic down-scaling of GABAergic synapses 3 days after denervation. Hence, additional pathological stimuli (*e.g.*, direct neuronal damage and/or cell death in the target region; c.f., Kinuchi et al., 2018) may account for maladaptive structural and functional homeostatic changes of GABAergic neurotransmission in denervated brain regions.

Acknowledgements

We thank Charlotte Nolte-Uhl and Simone Zenker for skillful assistance in tissue culturing. The work was supported by German-Israeli-Foundation (GIF G-1317-418.13/2015 to AV), Deutsche

Forschungsgemeinschaft (CRC 1080 to TD and AV), and “Nachlässe Held und Hecker” (to MF).

References

Arolfo, M.P., Brioni, J.D., 1991. Diazepam impairs place learning in the Morris water maze. Behav. Neural Biol. 55, 131–136.

Bannai, H., Levi, S., Schweizer, C., Inoue, T., Launey, T., Racine, V., Sibarita, J.B., Mikoshiba, K., Triller, A., 2009. Activity-dependent tuning of inhibitory neurotransmission based on GABAAR diffusion dynamics. Neuron 62, 670–682.

Barnes, S.J., Franzoni, E., Jacobsen, R.I., Erdelyi, F., Szabo, G., Clopath, C., Keller, G.B., Keck, T., 2017. Deprivation-Induced Homeostatic Spine Scaling in Vivo is Localized to Dendritic branches that have Undergone recent Spine loss. Neuron 96 (871–882), e875.

Becker, D., Zahn, N., Deller, T., Vlachos, A., 2013. Tumor necrosis factor alpha maintains denervation-induced homeostatic synaptic plasticity of mouse dentate granule cells. Front. Cell. Neurosci. 7, 257.

Becker, D., Deller, T., Vlachos, A., 2015. Tumor necrosis factor (TNF)-receptor 1 and 2 mediate homeostatic synaptic plasticity of denervated mouse dentate granule cells. Sci. Rep. 5, 12726.

Bliss, T.V., Collingridge, G.L., 2013. Expression of NMDA receptor-dependent LTP in the hippocampus: bridging the divide. Mol. Brain 6, 5.

Botta, P., Demmou, L., Kasugai, Y., Markovic, M., Xu, C., Fadok, J.P., Lu, T., Poe, M.M., Xu, L., Cook, J.M., Rudolph, U., Sah, P., Ferraguti, F., Luthi, A., 2015. Regulating anxiety with extrasynaptic inhibition. Nat. Neurosci. 18, 1493–1500.

Brioni, J.D., Nagahara, A.H., Mcgaugh, J.L., 1989. Involvement of the amygdala GABAergic system in the modulation of memory storage. Brain Res. 487, 105–112.

Bui, A.D., Nguyen, T.M., Limouse, C., Kim, H.K., Szabo, G.G., Felong, S., Maroso, M., Soltesz, I., 2018. Dentate gyrus mossy cells control spontaneous convulsive seizures and spatial memory. Science 359, 787–790.

Caroni, P., 2015. Regulation of Parvalbumin Basket cell plasticity in rule learning. Biochem. Biophys. Res. Commun. 460, 100–103.

Collinson, N., Kuenzi, F.M., Jarolimek, W., Maubach, K.A., Cothliff, R., Sur, C., Smith, A., Otu, F.M., Howell, O., Atack, J.R., Mckernan, R.M., Seabrook, G.R., Dawson, G.R., Whiting, P.J., Rosahl, T.W., 2002. Enhanced learning and memory and altered GABAergic synaptic transmission in mice lacking the alpha 5 subunit of the GABAA receptor. J. Neurosci. 22, 5572–5580.

Davis, M., 1979. Diazepam and flurazepam: effects on conditioned fear as measured with the potentiated startle paradigm. Psychopharmacology 62, 1–7.

Davis, G.W., 2006. Homeostatic control of neural activity: from phenomenology to molecular design. Annu. Rev. Neurosci. 29, 307–323.

Deller, T., Frotscher, M., Nitsch, R., 1995. Morphological evidence for the sprouting of inhibitory commissural fibers in response to the lesion of the excitatory entorhinal input to the rat dentate gyrus. J. Neurosci. 15, 6868–6878.

Dinocourt, C., Aungst, S., Yank, K., Thompson, S.M., 2011. Homeostatic increase in excitability in area CA1 after Schaffer collateral transection in vivo. Epilepsia 52, 1656–1665.

Essrich, C., Lorenz, M., Benson, J.A., Fritschy, J.M., Luscher, B., 1998. Postsynaptic clustering of major GABAA receptor subtypes requires the gamma 2 subunit and gephyrin. Nat. Neurosci. 1, 563–571.

Feng, G., Tintrup, H., Kirsch, J., Nichol, M.C., Kuhse, J., Betz, H., Sanes, J.R., 1998. Dual requirement for gephyrin in glycine receptor clustering and molybdoenzyme activity. Science 282, 1321–1324.

Froemke, R.C., 2015. Plasticity of cortical excitatory-inhibitory balance. Annu. Rev. Neurosci. 38, 195–219.

Fu, Y., Kaneko, M., Tang, Y., Alvarez-Buylla, A., Stryker, M.P., 2015. A cortical disinhibitory circuit for enhancing adult plasticity. elife 4, e05558.

Ge, Y., Kang, Y., Cassidy, R.M., Moon, K.M., Lewis, R., Wong, R.O.L., Foster, L.J., Craig, A.M., 2018. Clptm1 Limits Forward trafficking of GABAA Receptors to Scale Inhibitory Synaptic Strength. Neuron 97 (596–610), e598.

Germroth, P., Schwerdtfeger, W.K., Buhl, E.H., 1989. GABAergic neurons in the entorhinal cortex project to the hippocampus. Brain Res. 494, 187–192.

Germroth, P., Schwerdtfeger, W.K., Buhl, E.H., 1991. Ultrastructure and aspects of functional organization of pyramidal and nonpyramidal entorhinal projection neurons contributing to the perforant path. J. Comp. Neurol. 305, 215–231.

Granger, A.J., Nicoll, R.A., 2014. Expression mechanisms underlying long-term potentiation: a postsynaptic view, 10 years on. Philos. Trans. R. Soc. Lond. Ser. B Biol. Sci. 369, 20130136.

Griffen, T.C., Maffei, A., 2014. GABAergic synapses: their plasticity and role in sensory cortex. Front. Cell. Neurosci. 8, 91.

Gu, F., Parada, I., Shen, F., Li, J., Bacci, A., Graber, K., Taghavi, R.M., Scalise, K., Schwartzkroin, P., Wenzel, J., Prince, D.A., 2017. Structural alterations in fast-spiking GABAergic interneurons in a model of posttraumatic neocortical epileptogenesis. Neurobiol. Dis. 108, 100–114.

Harris, J.A., Westbrook, R.F., 1995. Effects of benzodiazepine microinjection into the amygdala or periaqueductal gray on the expression of conditioned fear and hypoalgesia in rats. Behav. Neurosci. 109, 295–304.

Hulme, S.R., Jones, O.D., Abraham, W.C., 2013. Emerging roles of metaplasticity in behaviour and disease. Trends Neurosci. 36, 353–362.

Joseph, A., Turrigiano, G.G., 2017. All for one but not one for all: Excitatory Synaptic Scaling and Intrinsic Excitability are Coregulated by CaMKIV, whereas Inhibitory Synaptic Scaling is under Independent Control. J. Neurosci. 37, 6778–6785.

Kinuchi, R., Hamanoue, M., Koshimoto, M., Kohsaka, S., Nakajima, K., 2018. Response of the GABAergic System to Axotomy of the Rat Facial Nerve. Neurochem. Res. 43, 324–339.

Kiss, E., Gorgas, K., Schlicksupp, A., Gross, D., Kins, S., Kirsch, J., Kuhse, J., 2016. Biphasic Alteration of the Inhibitory Synapse Scaffold Protein Gephyrin in early and late Stages of an Alzheimer Disease Model. Am. J. Pathol. 186, 2279–2291.

Kneussel, M., Brandstatter, J.H., Laube, B., Stahl, S., Muller, U., Betz, H., 1999. Loss of postsynaptic GABA(a) receptor clustering in gephyrin-deficient mice. J. Neurosci. 19, 9289–9297.

Lenz, M., Platschek, S., Priesemann, V., Becker, D., Willems, L.M., Ziemann, U., Deller, T., Muller-Dahlhaus, F., Jedlicka, P., Vlachos, A., 2015. Repetitive magnetic stimulation induces plasticity of excitatory postsynapses on proximal dendrites of cultured mouse CA1 pyramidal neurons. Brain Struct. Funct. 220, 3323–3337.

Lenz, M., Galanis, C., Muller-Dahlhaus, F., Opitz, A., Wierenga, C.J., Szabo, G., Ziemann, U., Deller, T., Funke, K., Vlachos, A., 2016. Repetitive magnetic stimulation induces plasticity of inhibitory synapses. Nat. Commun. 7, 10020.

Letzkus, J.J., Kampa, B.M., Stuart, G.J., 2006. Learning rules for spike timing-dependent plasticity depend on dendritic synapse location. J. Neurosci. 26, 10420–10429.

Letzkus, J.J., Wolff, S.B., Meyer, E.M., Tovote, P., Courtin, J., Herry, C., Luthi, A., 2011. A disinhibitory microcircuit for associative fear learning in the auditory cortex. Nature 480, 331–335.

Letzkus, J.J., Wolff, S.B., Luthi, A., 2015. Disinhibition, a Circuit Mechanism for Associative Learning and memory. Neuron 88, 264–276.

Lewis, D.A., 2014. Inhibitory neurons in human cortical circuits: substrate for cognitive dysfunction in schizophrenia. Curr. Opin. Neurobiol. 26, 22–26.

Long, Z., Medlock, C., Dzemidzic, M., Shin, Y.W., Goddard, A.W., Dydak, U., 2013. Decreased GABA levels in anterior cingulate cortex/medial prefrontal cortex in panic disorder. Prog. Neuro-Psychopharmacol. Biol. Psychiatry 44, 131–135.

Lopez-Bendito, G., et al., 2004. Preferential origin and layer destination of GAD65-GFP cortical interneurons. Cereb. Cortex 14, 1122–1133.

Luscher, C., Malenka, R.C., 2012. NMDA receptor-dependent long-term potentiation and long-term depression (LTP/LTD). Cold Spring Harb. Perspect. Biol. 4.

Maffei, A., Nataraj, K., Nelson, S.B., Turrigiano, G.G., 2006. Potentiation of cortical inhibition by visual deprivation. Nature 443, 81–84.

Maggio, N., Vlachos, A., 2014. Synaptic plasticity at the interface of health and disease: New insights on the role of endoplasmic reticulum intracellular calcium stores. Neuroscience 281, 135–146.

Marder, E., Goaillard, J.M., 2006. Variability, compensation and homeostasis in neuron and network function. Nat. Rev. Neurosci. 7, 563–574.

Mcnaughton, N., Morris, R.G., 1987. Chlordiazepoxide, an anxiolytic benzodiazepine, impairs place navigation in rats. Behav. Brain Res. 24, 39–46.

Melzer, S., Michael, M., Caputi, A., Eliava, M., Fuchs, E.C., Whittington, M.A., Monyer, H., 2012. Long-range-projecting GABAergic neurons modulate inhibition in hippocampus and entorhinal cortex. Science 335, 1506–1510.

Peng, Y.R., He, S., Marie, H., Zeng, S.Y., Ma, J., Tan, Z.J., Lee, S.Y., Malenka, R.C., Yu, X., 2009. Coordinated changes in dendritic arborization and synaptic strength during neural circuit development. Neuron 61, 71–84.

Peng, Z., Zhang, N., Wei, W., Huang, C.S., Cetina, Y., Otis, T.S., Houser, C.R., 2013. A reorganized GABAergic circuit in a model of epilepsy: evidence from optogenetic labeling and stimulation of somatostatin interneurons. J. Neurosci. 33, 14392–14405.

Pi, H.J., Hangya, B., Kvitsiani, D., Sanders, J.I., Huang, Z.J., Kepecs, A., 2013. Cortical interneurons that specialize in disinhibitory control. Nature 503, 521–524.

Pribiag, H., Stellwagen, D., 2014. Neuroimmune regulation of homeostatic synaptic plasticity. Neuropharmacology 78, 13–22.

Radhu, N., Garcia Dominguez, L., Farzan, F., Richter, M.A., Semeralul, M.O., Chen, R., Fitzgerald, P.B., Daskalakis, Z.J., 2015. Evidence for inhibitory deficits in the prefrontal cortex in schizophrenia. Brain 138, 483–497.

Rojas, D.C., Singel, D., Steinmetz, S., Hepburn, S., Brown, M.S., 2014. Decreased left perisylvian GABA concentration in children with autism and unaffected siblings. NeuroImage 86, 28–34.

Rowland, L.M., Edden, R.A., Kontson, K., Zhu, H., Barker, P.B., Hong, L.E., 2013. GABA predicts inhibition of frequency-specific oscillations in schizophrenia. J. Neuropsychiatry Clin. Neurosci. 25, 83–87.

Rubenstein, J.L., Merzenich, M.M., 2003. Model of autism: increased ratio of excitation/inhibition in key neural systems. Genes Brain Behav. 2, 255–267.

Sanger, D.J., Joly, D., 1985. Anxiolytic drugs and the acquisition of conditioned fear in mice. Psychopharmacology 85, 284–288.

Simbürger, E., Plaschke, M., Kirsch, J., Nitsch, R., 2000. Distribution of the receptor-anchoring protein gephyrin in the rat dentate gyrus and changes following entorhinal cortex lesion. Cereb. Cortex 10, 422–432.

Simbürger, E., Plaschke, M., Fritschy, J.M., Nitsch, R., 2001. Localization of two major GABA(a) receptor subunits in the dentate gyrus of the rat and cell type-specific up-regulation following entorhinal cortex lesion. Neuroscience 102, 789–803.

Sjostrom, P.J., Hausser, M., 2006. A cooperative switch determines the sign of synaptic plasticity in distal dendrites of neocortical pyramidal neurons. Neuron 51, 227–238.

Small, D.H., 2008. Network dysfunction in Alzheimer's disease: does synaptic scaling drive disease progression? Trends Mol. Med. 14, 103–108.

Soltesz, I., Smetters, D.K., Mody, I., 1995. Tonic inhibition originates from synapses close to the soma. Neuron 14, 1273–1283.

Steinberg, E.E., Christoffel, D.J., Deisseroth, K., Malenka, R.C., 2015. Illuminating circuitry relevant to psychiatric disorders with optogenetics. Curr. Opin. Neurobiol. 30, 9–16.

Steinmetz, C.C., Turrigiano, G.G., 2010. Tumor necrosis factor-alpha signaling maintains the ability of cortical synapses to express synaptic scaling. J. Neurosci. 30, 14685–14690.

Stellwagen, D., Malenka, R.C., 2006. Synaptic scaling mediated by glial TNF-alpha. Nature 440, 1054–1059.

Steward, O., 1994. Reorganization of Neuronal Circuitry Following Central Nervous

System Trauma: Naturally Occurring Processes and Opportunities for Therapeutic Intervention. In: Salzman, S.K., Faden, A.I. (Eds.), The Neurobiology of Central Nervous System Trauma. Oxford University Press, New York, pp. 266–287.
Tatti, R., Haley, M.S., Swanson, O.K., Tselha, T., Maffei, A., 2017. Neurophysiology and Regulation of the Balance between Excitation and Inhibition in Neocortical Circuits. Biol. Psychiatry 81, 821–831.
Tremblay, R., Lee, S., Rudy, B., 2016. GABAergic Interneurons in the Neocortex: from Cellular Properties to Circuits. Neuron 91, 260–292.
Turrigiano, G.G., 2008. The self-tuning neuron: synaptic scaling of excitatory synapses. Cell 135, 422–435.
Turrigiano, G., 2011. Too many Cooks? Intrinsic and Synaptic Homeostatic Mechanisms in Cortical Circuit Refinement. Annu. Rev. Neurosci. 34, 89–103.
Turrigiano, G.G., 2017. The dialectic of Hebb and homeostasis. Philos. Trans. R. Soc. Lond. Ser. B Biol. Sci. 372.
Tyagarajan, S.K., Ghosh, H., Yevenes, G.E., Imanishi, S.Y., Zeilhofer, H.U., Gerrits, B., Fritschy, J.M., 2013. Extracellular signal-regulated kinase and glycogen synthase kinase 3beta regulate gephyrin postsynaptic aggregation and GABAergic synaptic function in a calpain-dependent mechanism. J. Biol. Chem. 288, 9634–9647.
van Versendaal, D., Rajendran, R., Saiepour, M.H., Klooster, J., Smit-Rigter, L., Sommeijer, J.P., De Zeeuw, C.I., Hofer, S.B., Heimel, J.A., Levelt, C.N., 2012. Elimination of inhibitory synapses is a major component of adult ocular dominance plasticity. Neuron 74, 374–383.
Vlachos, A., Becker, D., Jedlicka, P., Winkels, R., Roeper, J., Deller, T., 2012a. Entorhinal denervation induces homeostatic synaptic scaling of excitatory postsynapses of dentate granule cells in mouse organotypic slice cultures. PLoS One 7, e32883.
Vlachos, A., Bas-Orth, C., Schneider, G., Deller, T., 2012b. Time-lapse imaging of granule cells in mouse entorhinohippocampal slice cultures reveals changes in spine stability after entorhinal denervation. J. Comp. Neurol. 520, 1891–1902.
Vlachos, A., Helias, M., Becker, D., Diesmann, M., Deller, T., 2013a. NMDA-receptor inhibition increases spine stability of denervated mouse dentate granule cells and accelerates spine density recovery following entorhinal denervation in vitro. Neurobiol. Dis. 59, 267–276.
Vlachos, A., Ikenberg, B., Lenz, M., Becker, D., Reifenberg, K., Bas-Orth, C., Deller, T., 2013b. Synaptopodin regulates denervation-induced homeostatic synaptic plasticity. Proc. Natl. Acad. Sci. U. S. A. 110, 8242–8247.
Vlachos, A., Reddy-Alla, S., Papadopoulos, T., Deller, T., Betz, H., 2013c. Homeostatic regulation of gephyrin scaffolds and synaptic strength at mature hippocampal GABAergic postsynapses. Cereb. Cortex 23, 2700–2711.
Wierenga, C.J., Wadman, W.J., 1999. Miniature inhibitory postsynaptic currents in CA1 pyramidal neurons after kindling epileptogenesis. J. Neurophysiol. 82, 1352–1362.
Williams, S.R., Mitchell, S.J., 2008. Direct measurement of somatic voltage clamp errors in central neurons. Nat. Neurosci. 11, 790–798.
Wolff, S.B., Grundemann, J., Tovote, P., Krabbe, S., Jacobson, G.A., Muller, C., Herry, C., Ehrlich, I., Friedrich, R.W., Letzkus, J.J., Luthi, A., 2014. Amygdala interneuron subtypes control fear learning through disinhibition. Nature 509, 453–458.
Yizhar, O., Fenno, L.E., Prigge, M., Schneider, F., Davidson, T.J., O'Shea, D.J., Sohal, V.S., Goshen, I., Finkelstein, J., Paz, J.T., Stehfest, K., Fudim, R., Ramakrishnan, C., Huguenard, J.R., Hegemann, P., Deisseroth, K., 2011. Neocortical excitation/inhibition balance in information processing and social dysfunction. Nature 477, 171–178.